Dependence of the atmospheric muon rate on the sea water depth with first KM3NeT data

The KM3NeT Collaboration[‡][*]

[‡] *https://www.km3net.org/km3net-author-list-for-icrc-2019*
E-mail: `lincetto@cppm.in2p3.fr`

The first detection units of the KM3NeT/ORCA and KM3NeT/ARCA neutrino telescopes have been deployed at the French and Italian sites in the Mediterranean Sea. The first collected data have been crucial to assess the detector performance and to establish the calibration procedures. The low-level data streams of the deployed ARCA and ORCA detection units, containing raw information on hits in coincidence between PMTs for each Digital Optical Module, have been analysed. The study of coincidence rates has been exploited to evaluate the dependence of the atmospheric muon rate as a function of the sea depth, which is found to be in good agreement with model predictions.

Corresponding authors: Simone Biagi[1], Rosa Coniglione[1], Jannik Hofestädt[2], Vladimir Kulikovskiy[3], Massimiliano Lincetto[†4], Karel Melis[5], Dorothea Samtleben[5,6]

[1] *INFN, Laboratori Nazionali del Sud, Via S. Sofia 62, Catania, 95123 Italy*

[2] *Friedrich-Alexander-Universität Erlangen-Nürnberg, Erlangen Centre for Astroparticle Physics, Erwin-Rommel-Straße 1, 91058, Erlangen, Germany*

[3] *INFN, Sezione di Genova, Via Dodecaneso 33, Genova, 16146 Italy*

[4] *Aix Marseille Univ, CNRS/IN2P3, CPPM, Marseille, France*

[5] *Nikhef, National Inst. for Subatomic Physics, PO Box 41882, Amsterdam, 1009 DB Netherlands*

[5] *Leiden University, Leiden Institute of Physics, PO Box 9504, Leiden, 2300 RA Netherlands*

[*]for collaboration list see PoS(ICRC2019)1177

[†]Speaker.

1. Introduction

KM3NeT is a network of neutrino detectors under construction in the depth of the Mediterranean Sea [1]. It will consists of two detectors, ARCA and ORCA, sharing the same detection technology and primarily aimed, respectively, to the search for astrophysical neutrino sources [2] and to the determination of the neutrino mass ordering through the study of atmospheric neutrino oscillations [3]. ARCA is located in Italy, off the coast of Capo Passero (Sicily) at a seafloor depth of 3450 m, and will instrument a volume of km^3 scale. ORCA is being built in France, off shore of Toulon at a depth of 2425 m, adopting a denser geometry for the instrumentation of a mass of 8 Mton of seawater.

KM3NeT detectors are built as three-dimensional arrays of Digital Optical Modules (DOMs). The DOM [4] consists of a glass sphere housing 31 80 mm PMTs and a front-end electronics whose purpose is the digitisation of the signals and the dispatch of the data to shore via the KM3NeT underwater network infrastructure. DOMs are connected in groups of 18 to form vertical lines, named Detection Units (DUs). ARCA and ORCA DUs have spacings between the DOMs of 36 m and 9 m respectively. The horizontal spacing between the DUs is of 90 m for ARCA and about 20 m for ORCA. The analysis presented here is based on the data from the first two ARCA DUs and the first ORCA DUs deployed in 2016 and 2017 across the two sites. In the following, the two detector configurations are referred to as ARCA2 and ORCA1.

One of the primary sources of background for deep water Cherenkov neutrino detectors is the flux of atmospheric muons from air-showers induced by the impact of cosmic rays with the upper layers of the atmosphere. Muons are an almost constant and well-known source of background that can be used for the monitoring of the detector performance and calibration. The first data from KM3NeT ARCA2 and ORCA1 allow to probe the muon flux in a depth range between 2232 and 3386 meters. This analysis is specifically focused on the dependence of the muon rate on the sea water depth. The used method exploits the multi-PMT technology of KM3NeT digital optical modules and the in-situ calibration procedures.

2. Data acquisition and processing

The signal from each PMT of a KM3NeT DOM is digitised by a custom electronic board [5]. When one or more photons impinge on the PMT. photocatode, the time of the leading edge and the time-over-threshold of the corresponding pulse are recorded with nanosecond accuracy. This information is referred to as a *L0 hit*. Hit data are grouped by each DOM in globally synchronous segments of 100 ms, called timeslices, and sent to shore. At the shore computing farm, a dedicated software assembles the *L0 timeslices* containing all hits from the detector during the same time segment. Timeslice data are further processed by the data filter and trigger algorithms. The first step in this pipeline is the building of *coincidences* on a 10-25 ns scale, which are the typical signature of the tightly time-correlated photons of Cherenkov emissions. Coincidence data are referred to as *L1 timeslices*. A further selection (L2) based on the opening angle between the PMTs detecting light in coincidence is performed and fed to the trigger algorithms. Space and time correlations between coincidences (and hits) on multiple DOMs are used to identify clusters of causally-connected photons compatible with the signature of track and shower signals. The

storage policy for timeslice data is configurable on a run basis. Tipically, L0 data are stored in short dedicated calibration runs, due to the large data volume produced. Coincidence (L1) data are instead continuously acquired with a configurable downsampling factor N, i.e. only one timeslice every N is written to permanent storage. A dedicated data stream including only coincidences above a minimum number of hits (*SN timeslices*) is dedicated to supernova detection [6].

3. Detector response and calibration

In addition to atmospheric muons, the other optical background sources for KM3NeT are ^{40}K-dominated radioactive decays in sea water and bioluminescence.

Individual PMT counting rates are dominated by radioactive decays, accounting for a $\sim 7\,\text{kHz}$ hit rate per PMT. Bioluminescence can produce occasional increases (up to the MHz level) and lasting up to several second. To prevent spurious data from these bursts to overload the data acquisition system, individual PMT acquisition is disabled whenever the hit rate evaluated on a timeslice basis exceeds a threshold of 20 kHz. The selection of hits in coincidence on a 10-15 ns time scale is an effective way of selecting multi-photon Cherenkov emissions over the floor of uncorrelated single photons from radioactive decays and bioluminescence. While these contributions can still produce coincidences, the distribution of the time differences between the hits will reflect their uncorrelated nature.

On the other hand, ^{40}K decays are also able to induce multiple Cherenkov photons that can be detected on a single DOM. In general, photons from a point-like emission occurring in the proximity of the DOM are expected to hit multiple DOMs simultaneously. The distribution of the time differences between the recorded hits in coincidence hence depends on the spread of the transit time distribution (TTS) of the PMT and acquisition electronic, measured to be 2.1 ns on average [7]. The ^{40}K coincidence signal is the main source for the detector in-situ calibration. The expected coincidence rate as a function of the PMT opening angle is estimated from detailed simulations [8]. This parameterisation and a nominal gaussian model for the transit time distribution are used to fit the PMT photon detection efficiencies and time offsets of the 31 individual PMTs. In this, information from all the 465 PMT pairs is exploited simultaneously. The calibration principle is outlined in figure 1, with reference to time difference distribution between hits in coincidence for a typical PMT pair.
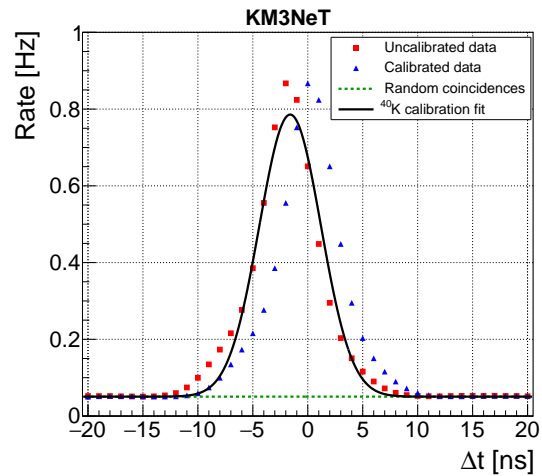

Figure 1: Distribution of time differences between hits in coincidence for one typical pair of adjacent PMTs, before (red) and after (blue) calibration. Only statistical errors are shown, which are smaller than the symbols. A peak due to genuine ^{40}K coincidences is observed above a flat background (green). The black line is a Gaussian fit of the calibration model to the uncalibrated data of all PMT pairs.

Contrarily to radioactive decays, atmospheric muons tend to produce long tracks across the detector volume. As a minimum ionising particle, an atmospheric muon has an average energy loss of $\sim 2\,\text{MeV} \cdot \text{cm}^{-1}$, producing tracks as long as 5 m per GeV of energy. Any track segment intercepting the DOM at the Cherenkov angle can potentially produce coincidences. Correlations between multiple DOMs allow the muon trigger to identify a track-like signature.

The number of photons in a coincidence is called *multiplicity* and is mostly dependent on the distance between the source of Cherenkov light and the DOM.

4. First KM3NeT data

In this work, the data acquired by ARCA2 between December 23, 2016 and March 2, 2017 and by ORCA1 between November 9, 2017 and December 13, 2017 are analysed. Being the first detector elements to be deployed, complete L1 timeslice data have been recorded for the ARCA2 data taking period. As for ORCA1, starting from November 23, 2017, the acquistion of L1 timeslices has been downsampled by a factor 20. The same data set has been used for both calibration and data analysis. For the purpose of calibration, data are processed in units of 6 hours in order to avoid statistical fluctuations of the fit results. The stability of the PMT efficiencies can be evaluated from Figure 2, where the relative deviation for each PMT photon detection efficiency from its all-time median is shown.
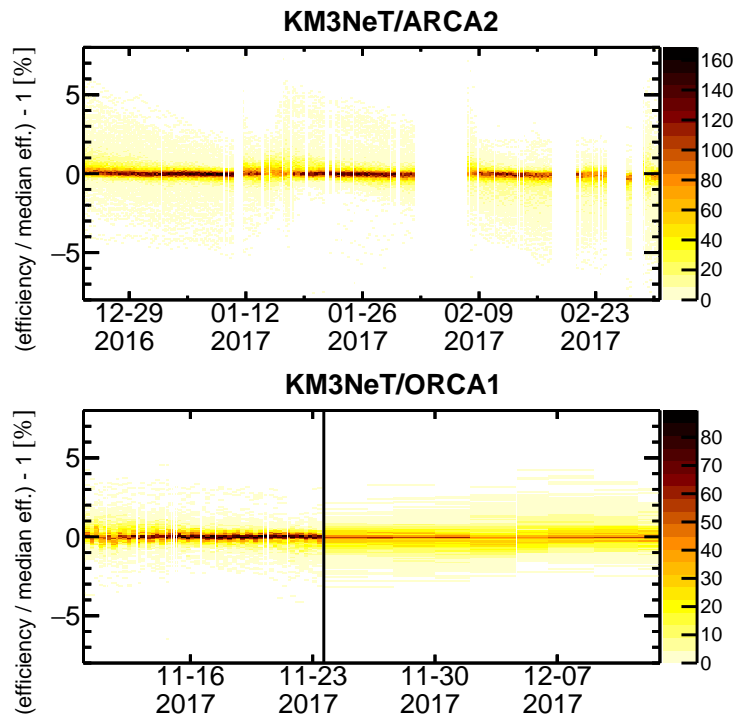

Figure 2: Deviation of the estimated photon detection efficiency for each PMT with respect to its global median efficiency by the ARCA2 and ORCA1 detectors as a function of time. The color scale indicates the number of PMTs in each bin. Vertical white bands reflect the periods without data-taking; the vertical black line represents the time at which the L1 data stream downscaling was introduced.

5. Coincidence rates

The study of the coincidence rate as a function of the multiplicity is an effective mean to evaluate the basic detector performance. In this work, the result of PMT calibration based on radioactive decays (dominating the low-multiplicity range) is used to correct a measurement of coincidences in the high-multiplicity range, which is a signature of atmospheric muons approaching the DOMs. The spectra of coincidence rates as measured for ARCA2 and ORCA1 detectors are shown in Figure 3. The random background has been subtracted with the same technique shown in Figure 1 for calibration, applied at a DOM level.
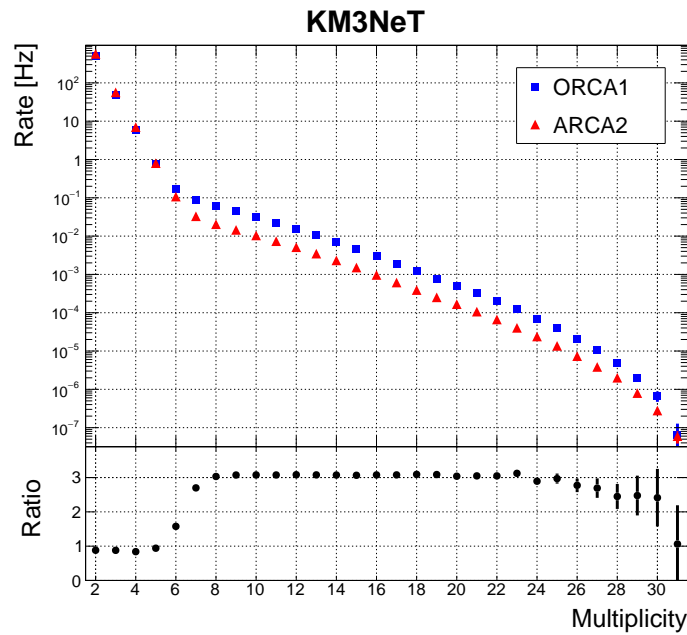

Figure 3: Top: coincidence rates as a function of the multiplicity for the ORCA1 and ARCA2 detectors averaged over all the DOMs of each detector. Bottom: ratio between ORCA1 and ARCA2 coincidence rates. Up to a multiplicity of six, the coincidence rate is dominated by ^{40}K decays. Above a multiplicity of seven, atmospheric muons dominate. Only statistical errors are shown.

Coincidence rates with multiplicity up to 4 are comparable between the two detectors as sea water salinity and the salt isotopic composition are independent of the site. The slightly higher rates observed in ARCA2 are a consequence of the lower efficiency observed for six out of eighteen DOMs in the single detection unit of ORCA1. The tail at high multiplicity shows a fixed ratio between the two detectors, reflecting the different rate of atmospheric muons due to the different average depths of the two detectors. The signal composed by the sum of coincidence rates above multiplicity 8 appears as a good candidate to probe the dependence of the atmospheric muon rate as a function of the sea water depth.

6. Efficiency correction

In order to correct the measured coincidence rates for the effect of the different PMT efficiencies of each DOM, two simulations of the detector response to atmospheric muons have been

performed. One simulation, *uniform*, uses a globally fixed PMT photon detection efficiency set to the overall mean value of the PMTs in the two detectors. A second one, *calibrated*, uses PMT efficiencies as calibrated according to the procedure described above. The MUPAGE [9] event generator is used to simulate (bundles of) muons on the surface of a volume surrounding the detector. The propagation of muons inside the detector volume is done with KM3 [10], a software based on tabulated results from a GEANT3.21 simulation of track and shower segments. KM3 comprises as well the parameterisation of the PMT sensitivity in terms of wavelength and incidence angle of the photon. The hits generated at KM3 level are further processed by custom KM3NeT software. The processing accounts for the (nominal or calibrated) photon detection efficiency, the PMT analog response, the emulation of the front-end electronics and the assembly of the data segments in simulated timeslices. Simulated run files are produced with a format identical to the one of the data acquisition system. The same analysis software can therefore be applied on data and Monte Carlo. After estimating the rates in the two simulations ($R_{\mathrm{uniform}}^{\mathrm{MC}}$ and $R_{\mathrm{calibrated}}^{\mathrm{MC}}$), the measured coincidence rates for multiplicities above 8 ($R_{\mathrm{measured}}^{\mathrm{data}}$) are corrected according to the following relation:

$$R_{\mathrm{corrected}}^{\mathrm{data}} = R_{\mathrm{measured}}^{\mathrm{data}} \cdot \frac{R_{\mathrm{uniform}}^{\mathrm{MC}}}{R_{\mathrm{calibrated}}^{\mathrm{MC}}} \, . \tag{6.1}$$

7. Depth dependence of muon-induced coincidence rates

Figure 4 shows the dependence on the sea water depth of the coincidence rates above multiplicity 8. The uncorrected data series (represented by blue hollow markers) show significant effects of the different PMT efficiencies between the DOMs.
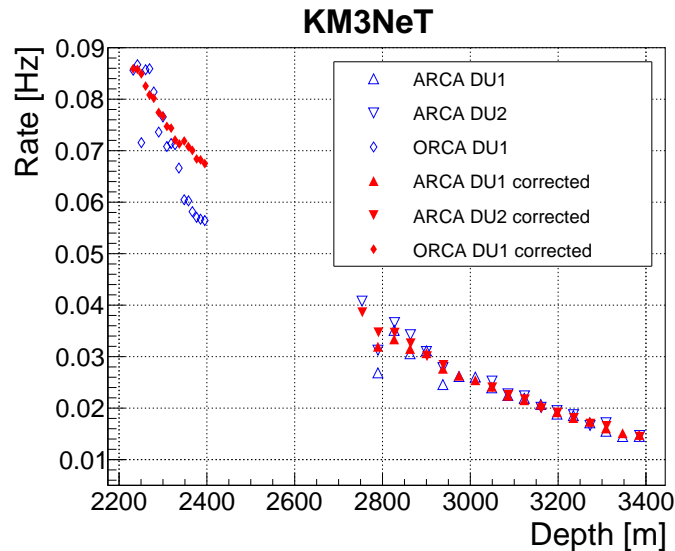

Figure 4: Multiplicity ≥ 8 coincidence rate of all DOMs as function of depth below the sea level. The coincidence rates for the ARCA2 and ORCA1 detectors are reported as measured (blue points) and after the correction for the PMT photon detection efficiencies (red points). Statistical uncertainties are included and smaller than markers.

The corrected rates are compared with a model of the muon flux in Figure 5. Data from the two ARCA DUs have been averaged at each depth, here expressed in *meters of water equivalent*. A fixed sea water density of $1.03 \times 10^3 \, \mathrm{kg \cdot m^{-1}}$ is considered. The muon flux to be compared is parameterised as follows:

$$I_\mu(d) = \frac{I_\mu(d, \theta = 0)}{C(d)} = \frac{A_1 \cdot e^{A_2 \cdot d} + A_3 \cdot e^{A_4 \cdot d}}{B_1 + B_2 \cdot d} \,, \tag{7.1}$$

$$A_1 = 1.31 \times 10^{-5} \, \mathrm{cm^{-2} s^{-1} sr^{-1}} \,, \ A_2 = -2.91 \times 10^{-3} \, \mathrm{m^{-1}} \,,$$

$$A_3 = 7.31 \times 10^{-7} \, \mathrm{cm^{-2} s^{-1} sr^{-1}} \,, \ A_4 = -1.17 \times 10^{-3} \, \mathrm{m^{-1}} \,,$$

$$B_1 = 4.16 \times 10^{-1} \, \mathrm{sr^{-1}} \,, \ B_2 = 1.07 \times 10^{-4} \, \mathrm{m^{-1} sr^{-1}} \,.$$

where the vertical depth-intensity relation $I_\mu(d, \theta = 0)$ is divided by a depth-dependent factor $C(d)$, accounting for the integration of the flux over the zenith angle. This simplified parametric formula is used to represent the detailed model elaborated by Bugaev et al. [11]. To this purpose, the A_i and B_j parameters have been estimated by fitting a numerical integration of the formulas provided in [12].

Assuming a fixed conversion between the muon flux at a given depth and the corresponding coincidence rate above multiplicity 8, the formula provided in Equation 6.1 has been fitter to the corrected rates through a normalisation factor R_0, as the only free parameter in the fit:

$$R(d) = R_0 \cdot I_\mu(d) \,. \tag{7.2}$$

The root-mean-square of the residuals of the fit is evaluated to be below 2%, reflecting the effectiveness of the calibration procedure used to correct the measured rates. The *uniform* simulation allow us to verify that the factor R_0 is constant within 4% between the two extremes of the depth range.

8. Conclusions

The first KM3NeT data collected with 2 DUs of the ARCA detector and 1 DU of the ORCA detector have been analysed. The data have been used to calibrate the detector in terms of PMT time offsets and photon detection efficiencies. Coincidence rates at high multiplicity have been measured as a probe of the Cherenkov signal induced by atmospheric muons. Using the Monte Carlo simulation based on the calibrated efficiencies, the measured rates have been corrected and compared with a model of the underwater muon flux. A good agreement of the depth-dependence relation is found between the data an the model.

References

[1] S. Adrián-Martínez et al. (KM3NeT Collaboration), *Letter of intent for KM3NeT 2.0*, J. Phys. G: Nucl. Part. Phys. **43** (2016) 084001.

[2] S. Aiello et al. (KM3NeT Collaboration), *Sensitivity of the KM3NeT/ARCA neutrino telescope to point-like neutrino sources*, Astropart. Phys. **111** (2019) 100–110.
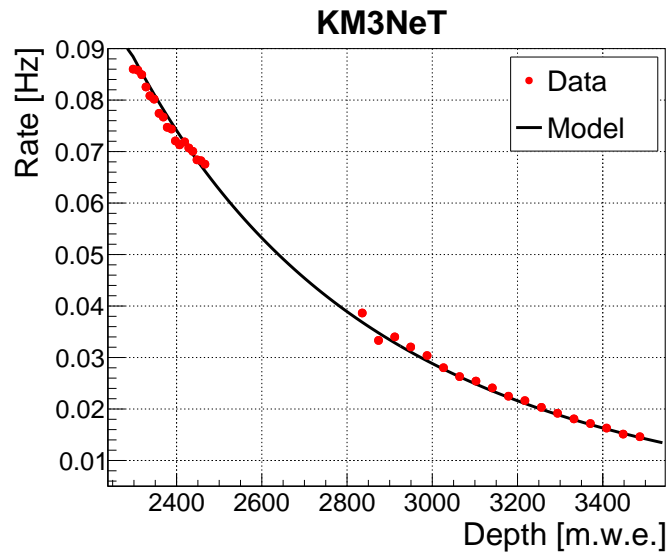
Figure 5: Efficiency-corrected ≥ 8 multiplicity coincidence rates measured with the ORCA1 and ARCA2 detectors as a function of depth below the sea level (red points), fitted with the Bugaev model of the atmospheric muon flux (continuous black line). The depth is expressed in meters of water equivalent (w.e.). Statistical uncertainties are included and smaller than markers.

[3] S. Adrián-Martínez et al. (KM3NeT Collaboration), *Intrinsic limits on resolutions in muon- and electron-neutrino charged-current events in the KM3NeT/ORCA detector*, JHEP **05** (2017) 008.

[4] R. Bruijn, D.van Eijk et al. (for the KM3NeT Collaboration), *The KM3NeT Multi-PMT Digital Optical Module*, PoS(ICRC2015)1157 (2015).

[5] S. Biagi and A. Orzelli (for the KM3NeT Collaboration), *The Central Logic Board and its auxiliary boards for the optical module of the KM3NeT detector*, JINST **9** (2014) C12033.

[6] M. Colomer Molla and M. Lincetto, EPJ Web Conf. **209** (2019) 01009. doi:10.1051/epjconf/201920901009

[7] S. Aiello et al. (KM3NeT Collaboration), *Characterisation of the Hamamatsu photomultipliers for the KM3NeT Neutrino Telescope*, JINST **13** (2018) P05035.

[8] M. Colomer *et al.* [KM3NeT Collaboration], PoS ICRC **2017** (2018) 983. doi:10.22323/1.301.0983

[9] Y. Becherini et al., *A parameterisation of single and multiple muons in the deep water or ice*, Astropart. Phys. **25** (2006) 1.

[10] A. Margiotta (for the ANTARES Collaboration), *Common simulation tools for large volume neutrino detectors*, Nucl. Instrum. Meth. **A725** (2013) 98.

[11] E.V. Bugaev et al., *Atmospheric muon flux at sea level, underground, and underwater*, Phys. Rev. D **58** (1998) 054001.

[12] S. I. Klimushin, E. V. Bugaev, and I. A. Sokalski, *On the parametrization of atmospheric muon angular flux underwater*, Phys. Rev. D **64** (2001) 014016.